Cancer Chemother Pharmacol (2010) 65:625–639
DOI 10.1007/s00280-009-1068-8

ORIGINAL ARTICLE

Comparative pharmacokinetics of RAD001 (everolimus) in normal and tumor-bearing rodents

Terence O'Reilly · Paul M. J. McSheehy · R. Kawai · O. Kretz · L. McMahon · J. Brueggen · A. Bruelisauer · H.-P. Gschwind · P. R. Allegrini · H. A. Lane

Received: 18 February 2009 / Accepted: 6 July 2009 / Published online: 27 September 2009

Abstract
Purpose Comparative pharmacokinetic (PK) analysis of the mTOR inhibitor RAD001 (everolimus) in rats and mice.
Methods Blood cell partitioning, plasma protein binding and PK parameters of RAD001 in blood and tissues (including brain) of both mice and rats were determined. PK modeling predicted plasma/blood and tumor levels from a variety of regimens and these were compared with the known human PK profile. DCE-MRI was used to compare tumor vascularity between mice and rats. Estimation of IC50 values in vitro and ED50 values in vivo were used to provide an indication of anti-tumor activity.
Results The PK properties of RAD001 differed between mice and rats, including erythrocyte partitioning, plasma protein binding, plasma/blood $t_{1/2}$, oral bioavailability, volume of distribution, tissue/tumor penetration and elimination. Modeling of tumor and blood/plasma PK suggested that in mice, multiple daily administrations result in a $\sim$2-fold increase in tumor levels of RAD001 at steady state, whereas in rats, a $\sim$7.9-fold increase would occur. Weekly high-dose regimens were predicted not to facilitate tumor accumulation in either species. Total tumor levels of RAD001 were four- to eight-fold greater in rats than in mice. Rat tumors had a >2-fold greater plasma content and permeability compared to mouse tumors, which could contribute to differences in tumor drug uptake. Maximal antitumor effects (T/C of 0.04–0.35) were observed in both species after daily administration with similar C_{max} and AUC values of unbound (free) RAD001. These free levels of RAD001 are exceeded in serum from cancer patients receiving clinically beneficial daily regimens. In rodents, brain penetration of RAD001 was poor, but was dose-dependent and showed over-proportional uptake in rats with a longer $t_{1/2}$ compared to the systemic circulation.
Conclusions The PK of RAD001 differed between mice and rats, with rats having a PK profile closer to that of humans. High intermittent doses of RAD001 may be more appropriate for treatment of brain tumors.

Keywords Everolimus · RAD001 · Pharmacokinetics · Mice · Rat · Tumor

Electronic supplementary material The online version of this article (doi:10.1007/s00280-009-1068-8) contains supplementary material, which is available to authorized users.

T. O'Reilly · P. M. J. McSheehy (✉)
Department of Oncology Research,
Novartis Institutes for BioMedical Research,
WKL-125.13.17, 4002 Basel, Switzerland
e-mail: paul_mj.mcsheehy@novartis.com

R. Kawai · O. Kretz · A. Bruelisauer · H.-P. Gschwind
Department of Drug Metabolism and Pharmacokinetics,
Novartis Pharma AG, Basel, Switzerland

L. McMahon
Department of Drug Metabolism and Pharmacokinetics,
Novartis Institutes for BioMedical Research,
East Hanover, NJ, USA

J. Brueggen · P. R. Allegrini
Department of Oncology Research, Novartis Institutes
for BioMedical Research, 4002 Basel, Switzerland

H. A. Lane
Basilea Pharmaceutica International AG,
Brenzacherstrasse 487, Basel, Switzerland

Present Address:
L. McMahon
Wyeth Medica Ireland, Newbridge, Co, Kildare, Ireland

Introduction

RAD001 (everolimus) is an orally active mTOR inhibitor currently under clinical testing for its utility, alone and in combination, as an anticancer agent. The target of this class of agents is mTORC1, a multi-functional signal transducing protein, which obtains signals from many upstream inputs, propagating the information via regulation of multiple downstream pathways (reviewed in [1]). Besides serving a key role in normal mammalian cell physiology, principally facilitating cell-cycle progression from G1-S phase, mTORC1 has been implicated in cancer [1–3]. Consequently, this target has received considerable attention as an anticancer approach leading to the clinical development of inhibitors of mTORC1 function [1, 4]. mTORC1 may also function in cancer cell resistance to several agents besides mTOR inhibitors [5]. RAD001 (everolimus) is an orally bioavailable mTORC1 inhibitor, which blocks mTORC1 activity via a complex with the immunophilin FKBP-12. mTORC1 inhibitors act directly on tumor cells inhibiting both in vitro and in vivo growth [1, 4], but such inhibitors also possesses anti-angiogenic activity [1, 4, 6–8]. Although the antitumor activity of RAD001 has been extensively profiled in mouse and rat tumor models [e.g. 6, 9–11] and is in extensive clinical testing [e.g. 12–15], little has been reported about the pharmacokinetics (PK) of RAD001 in mice, in contrast to rats [16, 17] and humans [reviewed in 18], including normal volunteers [19], transplant patients [20] and cancer patients [12, 14, 21]). The PK-pharmacodynamics (PD) of RAD001 in rats has been used to assist in the development and interpretation of clinically tested regimens [14, 15, 22]. In the present study, we compare the PK profile of RAD001 in immunocompromised BALB/c *nu/nu* (some bearing subcutaneous KB-31 tumors) and CD-1 mice (without tumors), with that of Sprague–Dawley, Wistar and Lewis rats, the latter bearing syngeneic CA20948 pancreatic tumors which were used previously to investigate the RAD001 PK/PD relationships [9]. Furthermore, the effect of various multiple treatments of RAD001 on plasma/blood and tumor PK were evaluated by the use of PK modeling. In addition, the vascularity of mouse and rat tumors is compared using non-invasive dynamic-contrast-enhanced magnetic resonance imaging (DCE-MRI). Together, these two approaches show important differences between mice and rats for the overall PK of RAD001 in rodents.

Materials and methods

Materials

RAD001 (MW 958.2) dry powder was obtained from the Chemical Department Novartis Pharma AG, Basel. [^{3}H]RAD001 (40-*O*-(2-Hydroxy-[1,2-^{3}H]ethyl)rapamycin) was prepared at Novartis AG, Basel (specific radioactivity approximately 58 mCi/mg [2.15 GBq/mg] or 55.7 mCi/mmol [2.06 TBq/mmol]). Preparation of RAD001 for in vivo use is described below.

Cell culture materials were from Integra BioSciences (Wallisellen, Switzerland). Liquid media, fetal bovine serum (FBS) and media additives were from Life Technologies (Basel, Switzerland). Human cervical tumor cells, designated KB-31 and KB-8511 were obtained from Dr. R. M. Baker, Roswell Park Memorial Institute (Buffalo, NY, USA). B16/BL6 murine melanoma cells were obtained from Dr I Fidler, MD Anderson Cancer Center, Dallas, TX. Human lung A-549, NCI H-596, NCI H-520 and colon HCT-116, HT-29 cells were obtained from the American Type Culture Collection. The cells were cultured in vitro according to the recommendations of the suppliers.

Animal strains used

Healthy, pathogen-free female BALB/c *nu/nu* (nude) mice and male Lewis rats were obtained from Iffa Credo (L'Arbesque, France). Female Sprague–Dawley and male Wistar rats, and male and female CD-1 mice were obtained from Charles River, Germany. Mice (CD-1) and rats were housed in conventional facilities and nude mice housed under optimal hygienic condition facilities (10 mice/Type III cage). All animals received food and water ad libitum. All experimental procedures involving animals were approved by the Kantonales Veterinäramt Basel-Stadt, Switzerland (Permit No. 1402, 1551, and 1672). The body weight of the BALB/c nude mice used in this study was on average 21 g with a range of 19–22 g; the CD-1 male mice mean 28.6, range 24.6–32.5 g; and CD-1 female mean 23.4, range 20.0–28.3 g; Wistar rats weighed 290–325 g (mean 300 g), Lewis rats 242–286 g (mean 256 g) and Sprague–Dawley 280–302 g (mean 286 g). Female Harlan nude mice (20–30 g) were bred in house. Female Harlan nude Rowett rats weighed 250–320 g.

Distribution of [^{3}H]RAD001 between erythrocytes and diluted plasma

[^{3}H]RAD001 was incubated in fresh murine blood at 5–5,000 ng/mL at 37°C for 5 min followed by centrifugation at 1,600 × *g* for 2 min for the separation of plasma from blood cells. A second procedure involved suspending erythrocytes from mice in diluted plasma at 0.1, 0.5, 1, 2, 5, 7.5, 10, 20, 30, 40 and 60% of the normal hematocrit. The erythrocyte suspension, spiked with 10 ng/mL [^{3}H]RAD001, was incubated at 37°C for 5 min followed by centrifugation at 1600*g* for 2 min for the separation of the supernatant from erythrocytes. The radioactivity in each fraction was determined by

liquid scintillation. Analogous methods have already been described [17].

Preparation of s.c. transplanted tumors

Human tumor cells, designated KB-31, were obtained from Dr. R. M. Baker, Roswell Park Memorial Institute (Buffalo, NY, USA). The cells were cultured in vitro and used to establish subcutaneous tumors in BALB/c nude mice. Tumors were established by subcutaneous injection of cells (minimum 2×10^6 cells in 100 μL PBS) in female BALB/c nude carrier mice (4–8 mice). The resulting tumors were serially passaged for a minimum of two consecutive transplantations prior to start of treatment. Tumor fragments (approx. 40 mg) were implanted s.c. into the left flank of animals with a 13-gauge trocar needle under Forene (Abbott, Switzerland) anesthesia. The CA20948 pancreatic tumors have not been isolated as a cell line and consequently a suspension of cells from donor rats was injected subcutaneously into the left flank of rats as previously described [9]. Other tumor models used for DCE-MRI (see below) were prepared as previously described [23, 24].

For PK studies, mice and rats were treated with RAD001 when the tumors had reached a volume of approximately 300 and 1,000 mm^3, respectively.

Preparation of RAD001 for administration to mice and rats

For p.o. administration, a microemulsion of 2% w/v RAD001, or RAD001-free microemulsion vehicle (obtained from Pharmaceutical Development, Novartis Pharma AG, Basel, Switzerland) was diluted with 5% w/v glucose in pyrogen-free water to administer the required dose in a volume of 10 mL/kg for p.o. administration; some studies used RAD001 diluted with 0.9% w/v NaCl. Formulation of RAD001 for i.v. administration involved dissolving dry substance in Cremophor EL-ethanol [2/1 w/w], and diluting this 1:5 with 5% w/v glucose in water for injection. The required i.v. dose of RAD001 was administered at 1 mL/kg. RAD001 was administered p.o. by gavage using a bead-tipped, curved cannula, or intravenously via the tail vein using plastic syringes fitted with 23 g (mice) or 20 g (rats) needles.

Tissue sampling

At the allotted times, blood samples were withdrawn into syringes containing EDTA (~0.5% w/v final) and, when needed, plasma prepared by centrifugation (10,000×*g*, 5 min). Blood (or plasma), muscle, skin and depending upon the experiment, tumor, kidney, lung, brain, spleen, gastrointestinal tract, liver and fat were obtained at various times after p.o. administration of RAD001. Tissues were weighed and frozen in liquid nitrogen (stored at −80°C).

Administration of [^{3}H]RAD001

[^{3}H]RAD001 was mixed with non-radiolabeled RAD001 to obtain the appropriate radioactive dose (88 μCi/kg for the dose–response curve and 200 μCi/kg for the time course study). Consequently, the specific radioactivity differed between the preparations. For the dose–response of brain penetration, RAD001 was formulated in a mixture of PEG200: ethanol, 40:10 (v/v). For the kinetic study, RAD001 was first solubilized in a mixture of 65% Cremophor®/35% ethanol and diluted with saline (at a ratio of 1–2.6, v/v). The preparations were checked for purity by HPLC. Evaluation of the chromatograms showed a radiochemical purity of >98%. At the designated times, animals were exposed to isoflurane anesthesia, and then were exsanguinated by bleeding from the vena cava. Thereafter, tissue aliquots were collected into heparin-containing vials. Determination of parent drug in whole blood, plasma and brain samples was performed using HPLC reverse isotope dilution analysis (LC-RID) [see Supplemental Material (SM)].

The amount of radioactivity in each sample was measured by liquid scintillation counting; samples were dissolved directly in scintillation fluid or processed by digestion with Soluene®: six aliquots of the drug formulation (5 μL) were added to 10 mL of Lumasafe® (Lumac Ltd, Landgraaf, NL) in 23 mL antistatic polyethylene vials (Canberra Packard, Meriden, CT). Whole blood, blood cells and plasma (aliquots of 50 μL) were pipetted into 6 mL glass vials, dried at 80°C for 1.5 h and incubated with 0.1 mL of aqueous NaOH (0.01 M) at room temperature for 2 h. Thereafter, 0.5 mL of Solutron® (Kontron Instruments, Zurich, CH)-isopropanol (1:2 v/v) were added and the samples were kept at room temperature overnight. Finally, 0.2 mL hydrogen peroxide (30%) and 7 mL Lumasafe®-HCl 0.7 M (9:1, v/v) were added. Brain tissue (two aliquots of 20–50 mg) was weighed in glass vials, dried at 50°C under vacuum overnight and was incubated with 0.1 mL of aqueous NaOH (0.01 M) at room temperature for 4 h. Thereafter, 0.5 mL of Solutron® was added and the samples were kept at room temperature overnight. Finally 5 mL Lumasafe®-HCl 0.7 M (9:1, v/v) was added.

Before counting, all samples were kept in the counter at ambient temperature overnight. For the counting, Tri-Carb liquid scintillation spectrometers, Models 2200CA or 2500TR (Canberra Packard, Meriden, CT) were used. Quench correction was performed by the external standard ratio (ESR) method, with radiolabeled hexadecane as the standard. All instruments were checked daily with a set of quenched tritium standards (Canberra Packard, Meriden,

CT). Measured values from spiked samples were within the range of 100 ± 3% of their true values.

Determination of metabolites in urine and feces

Pools of feces and urine (0–24, 24–48 and 48–72 h) were prepared. Urine was freeze-dried and redissolved in 0.01 M ammonium acetate (pH 6.5) prior to HPLC analysis. Feces were extracted three times with methanol, and the supernatants centrifuged for 10 min (3,000 rpm, 5°C) and then evaporated under reduced pressure. The remaining pellets were resuspended and the pH adjusted to 3.5–4 with acetic acid. The overall recovery from feces was between 60 and 80% of the dose. Extracts were directly injected into the HPLC system for analysis.

Determination of RAD001 concentrations in tissues and plasma

RAD001 concentration was determined using HPLC/Mass spectrometry (see SM).

Calculation of pharmacokinetic parameters

Areas under the plasma/tissue concentration versus time curves (AUC) were calculated from the mean values by a non-compartmental method using the WinNonlin Standard edition software (Version 3.1, Pharsight). Maximum concentrations (C_{max}) and time to reach C_{min} were determined by inspection of the data. Non-compartmental analysis was used to initially characterize single-administration PK profiles in plasma and tumor and to provide estimates of kinetic parameters for further modeling. The choice of model to ultimately use was based upon correlation coefficients, Akaike Information Criterion (AIC) and Schwarz Criterion (SC), determination of F-ratios [25], and the overall coefficient of variation of the estimates of AUC, C_{max} and Clearance (CL). Based upon these, 1 or 2-compartmental models were used to simulate RAD001 levels in blood and tumor tissue. The models were then used to estimate the plasma and tumor levels of various multiple treatments.

Evaluation of the antitumor activity of RAD001 in immunocompromised mice bearing xenografted tumors

Female BALB/c nude mice bearing s.c. tumors originating from HCT-116 colon, KB-31 or KB-8511cervical, A-549, NCI H-596 or NCI H-520 lung tumor cells, and B16/BL6 melanoma in syngeneic C57BL6 mice, were treated with a variety of RAD001 doses (0.5–10 mg/kg, once daily, p.o.) when tumors reached a mean volume of 100 mm^3. Dose–response curves were generated and the ED_{50} values estimated by fitting Hill Plot functions to the data. The maximally tolerated dose of RAD001 is >60 mg/kg p.o., once per day in mice and >20 mg/kg, p.o., once per day in rats (data not shown). In all studies, RAD001 treatment was well tolerated, producing less than 10% body weight loss (data not shown).

Dynamic contrast-enhanced magnetic resonance imaging (DCE-MRI)

Animals were anaesthetized using 1.5% (v/v) isoflurane (Abbott, Cham Switzerland) in a 1:1 mixture of O_2/N_2 and placed on an electrically warmed pad for cannulation of one of the two tail-veins using a 30-gauge needle attached to an infusion line of 30 cm and volume 80 μL to permit remote administration of the contrast agent. The animals were positioned on a cradle in a supine position inside the 30 cm horizontal bore magnet and were anaesthetized with 1.5% (v/v) isoflurane in a 1:1 mixture of O_2/N_2 administered with a facemask (flow-rate: 0.7 L/min). Body temperature was maintained at 37 ± 1°C using warm airflow (monitored with a rectal probe). MRI experiments were performed on a Bruker DBX 47/30 spectrometer (Bruker Medical, Fällanden, CH) at 4.7 T equipped with a self-shielded 12 cm bore gradient system as previously described.

The contrast agent Vistarem, P792 (Guerbet, Paris, France) was injected after seven baseline acquisitions as a bolus (50 μL/s) via the catheterized tail vein. The Vistarem concentration map in tissue $C_m(t)$ was calculated by

$$C_m(t) = (R_1(t) - R_{10})/r_1$$

where $R_1(t) = 1/T_1(t)$, relaxivity r_1 was 10 s/mM for Vistarem at 4.7 T (personal communication Guerbet) and R_{10} is the mean baseline relaxation rate, i.e. the mean of the seven scans before Vistarem injection.

A two-compartment model was applied for measurement of tumor vascular permeability (K^{trans}), extracellular leakage space (V_e) and plasma volume (V_p) as previously described [23]. For data analysis, the entire visible tumor on the MR image was included into the region of interest.

Results

Blood cell distribution and plasma protein binding

Erythrocyte partitioning and plasma protein binding in mouse blood

The distribution of [^{3}H]RAD001 between blood cells and plasma was essentially concentration-independent over the range 5–5,000 ng/mL. The majority of the test compound was located in the plasma compartment, with the fraction

of [^{3}H]RAD001 in plasma amounting to 98 ± 4%, suggesting only about 2% of RAD001 blood levels was present in erythrocytes, in strong contrast to the erythrocyte partitioning occurring in rats (60%) and humans (80%) [17]. Plasma protein binding of [^{3}H]RAD001 was investigated with the erythrocyte partitioning method, which estimated 99.9% binding in mouse plasma (for details see Figure SM1 and Tables SM1–SM3). In contrast, plasma protein binding in rats and humans has been reported to be markedly lower at 92 and 75%, respectively [17].

RAD001 pharmacokinetics in mice

Non-tumor bearing BALB/c nude mice

Following oral administration of RAD001 (5 mg/kg once) blood and tissue levels were determined by HPLC/MS, and data are presented in Table 1 (see also Figure SM2). The compound was orally bioavailable and the C_{max} in blood (~4,530 ng/mL) occurred 1 h post administration. RAD001 was detected in blood up to 24 h (C_{24h} ~115 ng/mL), with an apparent $t_{1/2}$ of ~4.3 h and an $AUC_{0–24h}$ of ~29,800 ng h/mL. RAD001 was detected in all tissues, with C_{max} occurring at 1 h, apart from the gastrointestinal tract (0.5 h) and skin (6 h). C_{max} values ranged from ~3,961 ng/g (gastrointestinal tract) to ~69 ng/g (brain). RAD001 was detected in all tissues up to 24 h (C_{last} ranging from ~68 ng/g in the skin to 5 ng/g in brain). The $t_{1/2}$ in tissues ranged from ~4.0 h (gastrointestinal tract) to ~9.6 h (skin) and the $AUC_{0–24h}$ values ranged from ~19,450 ng h/mL (gastrointestinal tract) to ~560 ng h/mL (brain). Based upon blood cell partitioning, the estimate of the plasma fraction C_{max} is ~4,440 ng/mL, and based upon the plasma protein binding capacity, the plasma free-fraction was estimated to be C_{max} of ~4.4 ng/mL. When using the free fraction in plasma, mouse K_p (tissue penetration) values (Table 2) are comparable with those of the rat (see below; Tables 3, 4), although tissue-specific differences occur. This demonstrates the significant influence of differences in the protein binding of RAD001.

Non tumor-bearing CD-1 mice

Oral administration of [^{3}H]RAD001 (0.9 mg/kg once) yielded C_{max} and AUC of ~489 ng/mL, and ~4,130 nmol h/mL, respectively, and by the i.v. route yielded C_{max} and $AUC_{0–24h}$ of ~3,814 ng/mL and ~36,699 ng h/mL, respectively (Fig. 1a). Therefore, oral absorption of the parent compound and/or its metabolites was estimated at about 13% of the dose when evaluating C_{max} levels in blood and 11% when considering AUC. Systemic exposure to metabolites in mice was estimated to be low as almost all the circulating radioactivity was found to be unchanged RAD001. Irrespective of the administration route, the excretion of radioactivity was rapid and virtually complete with almost the entire dose excreted within 48 h (i.v. and p.o. >96% of the dose). Very low amounts of radioactivity were recovered between Day 4 and 7 (i.v. <0.5% and p.o. <0.1% of the administered dose). Excretion occurred almost exclusively within the feces (>95% of the dose) (Fig. 1b, c). The formation of tritiated water in urine during the time period 48–72 h was negligible indicating that the position of the ^{3}H-radiolabel in the RAD001 molecule ("ring" labeled) was (metabolically) stable in mice (data not shown).

As part of long-term toxicity studies, the PK of RAD001 in CD-1 mice was determined for various doses after 13 and 104 weeks of daily, p.o. administration (Fig. 2). The data indicated linear dose-dependent changes in C_{max} and AUC over the dose range of 0.15–15 mg/kg in both female and male mice at the end of 13 weeks (Fig. 2a, c), and the AUC on male mice after 104 weeks (Fig. 2d). However, in the longer experiment, where the doses 0.1, 0.3 and 0.9 mg/kg/day were administered, although the AUC of RAD001 in male mice remained linear over the dose range studied, quadratic curves better fit the dose–response of the AUC data for female mice, and for the C_{max} dose–response of both genders (Fig. 2b, d). However, owing to the sparse data, the curve fits should not be over-interpreted.

Tumor-bearing BALB/c nude mice

BALB/c nude mice with s.c. KB-31 human tumors were administered RAD001 (5 mg/kg once p.o.) and plasma, tumors, skin and muscle obtained up to 72 h thereafter. The compound was orally bioavailable and the plasma and muscle C_{max} (~2,513 ng/mL, ~144 ng/g, respectively) were at 1 h but delayed in tumor and skin to 2 h (Table 2, Figure SM2). RAD001 was detectable in all tissues 72 h after administration (not shown). Elimination from tumor ($t_{1/2}$) was apparently slower (~16 h) than for plasma, skin or muscle (~7.5, ~9, and ~10 h, respectively). When using unbound RAD001 levels in blood, K_p values based upon C_{max}, C_{24h} or $AUC_{0–24h}$ were high (Table 1), but were generally lower than those of rats (see below, Table 3, Figure SM6), although some overlap in values occurred. However, similar to that reported for rats [17], mouse K_p values were not constant over time, increasing late post RAD001 administration although decreasing as related to plasma concentration during the elimination phase (see Figure SM2).

Modeling of RAD001 PK in tumor-bearing mice

Through a re-iterative process, a one-compartment PK model was used to describe RAD001 in plasma and a two-compartment model for the tumor PK in mice

Table 1 Pharmacokinetic parameters of RAD001 in tissues of female BALB/c nude mice following a single RAD001 administration

	Tissue compartment									
	Blood	GI tract	Muscle	Kidney	Lung	Brain	Skin	Spleen	Liver	Fat
T_{max} (h)	1	0.5	1	1	1	1	6	1	1	1
C_{max} (ng/mL or ng/g)	4,530 ± 876	3,961 ± 1,139	262 ± 71	1,190 ± 213	1,823 ± 268	69 ± 29	255 ± 64	1,060 ± 219	1,380 ± 385	504 ± 168
C_{max}/D	906	792	52	238	364	14	51	212	276	101
T_{last} (h)	24	24	24	24	24	24	24	24	24	24
C_{last} (ng/mL or ng/g)	115 ± 25	31 ± 4	24 ± 5	42 ± 6	56 ± 11	5 ± 1	68 ± 17	29 ± 4	37 ± 6	32 ± 8
C_{min}/D	23	6	5	8	11	1	14	29	7	6
$t_{1/2}$ (h)	4.3	4.0	5.8	5.3	4.7	6.0	9.6	4.8	5.2	7.3
AUC_{0-24h} (ng h/mL)	29,868	19,447	3,147	8,233	12,956	561	4,118	7,152	8,548	3,581
AUC_{0-24h}/D (ng h/mL)/dose)	5,974	3,889	629	1,647	2,591	112	824	1,430	1,710	716
$C_{max\ tissue}/C_{max\ blood}$		0.87	0.06	0.26	0.40	0.02	0.06	0.23	0.30	0.11
$C_{last\ tissue}/C_{last\ blood}$		0.27	0.21	0.37	0.49	0.04	0.59	0.25	0.32	0.28
AUC_{tissue}/AUC_{blood}		0.65	0.11	0.28	0.43	0.02	0.14	0.24	0.29	0.12
Estimates using free RAD001 levels in blood										
$C_{max\ tissue}/C_{max\ blood\ (unbound)}$		892	60	270	83	16	58	241	314	114
$C_{last\ tissue}/C_{last\ blood\ (unbound)}$		275	213	373	497	44	603	257	328	284
$AUC_{tissue}/AUC_{blood\ (unbound)}$		664	108	281	443	19	141	244	292	122

Female BALB/c nude mice were administered a single administration of RAD001 at 5 mg/kg p.o.. Plasma and tissues were obtained at various time points following administration, and RAD001 levels determined using HPLC/MS. AUC and $t_{1/2}$ values were calculated by non-compartmental analysis of extravascular dosing (WinNonlin) using mean values. C_{max} and t_{max} were determined by inspection of the data. The estimates of the unbound (free) fraction in mouse plasma were based upon the total RAD001 level which is 2% partitioned into erythrocytes and 99.9% bound to plasma proteins. Therefore, the C_{max}, C_{min} and AUC_{0-24h} of unbound RAD001 were estimated to be 4.4, 0.1 ng/mL, and 29.3 ng h/Ml, respectively. Where possible, data are expressed as mean ± SEM, $n = 4$. D is the RAD001 dose 5 mg/kg

Table 2 Pharmacokinetic parameters of RAD001 in KB-31 tumor xenograft-bearing BALB/c nude mice

	0–24 h				0–72 h			
	Blood	Tumor	Muscle	Skin	Blood	Tumor	Muscle	Skin
T_{max} (h)	1	2	1	2	1	2	1	2
C_{max} (ng/mL or ng/g)	2,513 ± 273	102 ± 17	144 ± 12	71 ± 12	2,513 ± 273	102 ± 17	144 ± 12	71 ± 12
C_{max}/D	503	20	29	14	502	20	19	14
T_{last} (h)	24	24	24	24	72	72	72	72
C_{last} (ng/mL or ng/g)	128 ± 28	45 ± 8	25 ± 4	13 ± 2	11 ± 7	15 ± 7	1.4 ± 0.6	2.6 ± 1.6
C_{min}/D	26	9	5	3	2.2	3.1	0.28	0.52
$t_{1/2}$ (h)	5.4	21.8	13.1	7.1	7.5	16.1	9.0	9.7
AUC (ng h/mL)	19,415	1,639	1,372	992	20,434	2,589	1,659	1,183
AUC/D (ng h/mL)/dose	3,883	328	274	198	4,087	518	332	237
$C_{max\ tissue}/C_{max\ blood}$		0.04	0.06	0.03		0.04	0.06	0.03
$C_{last\ tissue}/C_{Last\ blood}$		0.35	0.20	0.10		0.12	0.01	0.02
AUC_{tissue}/AUC_{blood}		0.08	0.07	0.05		0.13	0.09	0.06
Estimates using free RAD001 levels in blood								
$C_{max\ tissue}/C_{max\ blood\ (unbound)}$		41	57	28		41	57	28
$C_{last\ tissue}/C_{last\ blood\ (unbound)}$		352	195	102		117	11	20
$AUC_{tissue}/AUC_{blood\ (unbound)}$		84	71	51		133	85	61

Female BALB/c nude mice bearing s.c. KB-31 xenotransplants of approximately 300 mm^3 were administered a single p.o. dose of 5 mg/kg RAD001. Plasma and tissues were obtained at various time points following administration, and RAD001 levels determined using HPLC/MS. AUC and $t_{1/2}$ values were calculated by non-compartmental analysis of extravascular dosing (WinNonlin) using mean values. C_{max} and t_{max} were determined by inspection of the data. Data are expressed as mean ± SEM, $n = 4$. D is the RAD001 dose in mg/kg

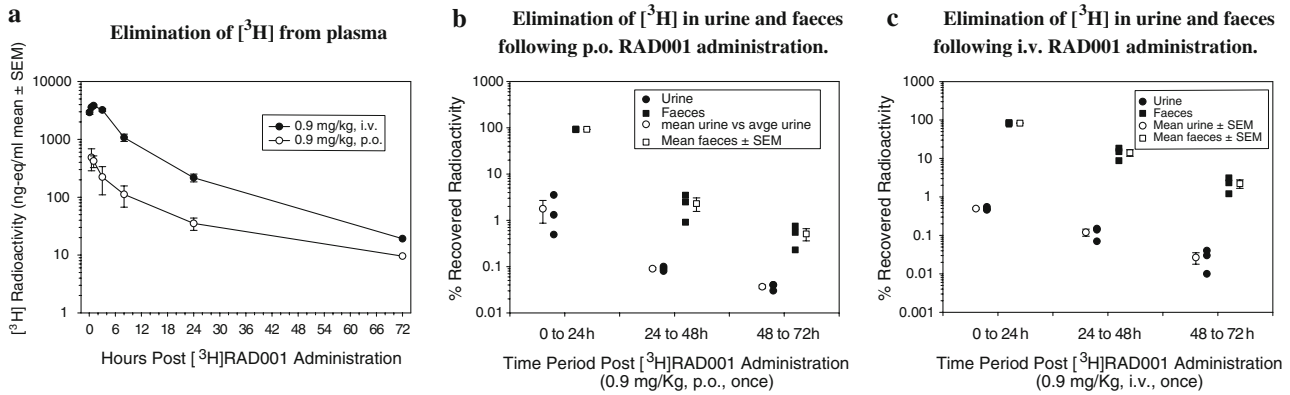

Fig. 1 Excretion of [^{3}H]RAD001 in non-tumor bearing CD-1 male mice. The extent of absorption, ^{3}H-kinetics in plasma (**a**) and excretion of total ^{3}H-radioactivity were investigated in mice after a single p.o. (**b**) or i.v. (**c**) administration of 0.9 mg/kg ^{3}H-labeled RAD001. The test compound was formulated in Cremophor EL-ethanol/NaCl 0.9% (w/v) (1/2.6, v/v) (i.v. route) or in microemulsion diluted 1/20 (v/v) with isotonic saline (p.o. route). Parameters estimated from non-compartmental analysis of the data obtained from i.v. administration include: C_{max} 3,814 ng/mL, $AUC_{0–24h}$ 37,657 ng h/mL, CL 0.79 mL/(min kg); $t_{1/2}$, 9.8 h, and V_{ss} 0.42 L/kg

(Table SM4 and Figures SM4 and SM5). The model predicted that RAD001, administered at 5 mg/kg, p.o. once per day, would accumulate slightly in blood with C_{max} values of approximately ∼2,625 ng/mL and C_{min} of ∼77 ng/mL after 6 days of treatment, representing a slight decrease in C_{min} and a slight increase in C_{max} over the measured levels (see Table SM4). After 6 days of treatment, tumor levels with this regimen produced tumor C_{max} and C_{min} values of ∼169 and ∼87 ng/g, respectively, approximately a 1.7- and 1.9-fold increase over the measured levels (see Table 2). Modeling of 5 or 20 mg/kg once per week indicated high C_{max} levels in plasma (∼2,559 and ∼10,237 ng/mL, respectively) and tumor (93 and 371 ng/g, respectively), but low C_{min} levels in plasma and tumor (∼0.7 and ∼2.6 ng/g, respectively) just prior to the next administration (Table SM4 and Figure SM5). The once per

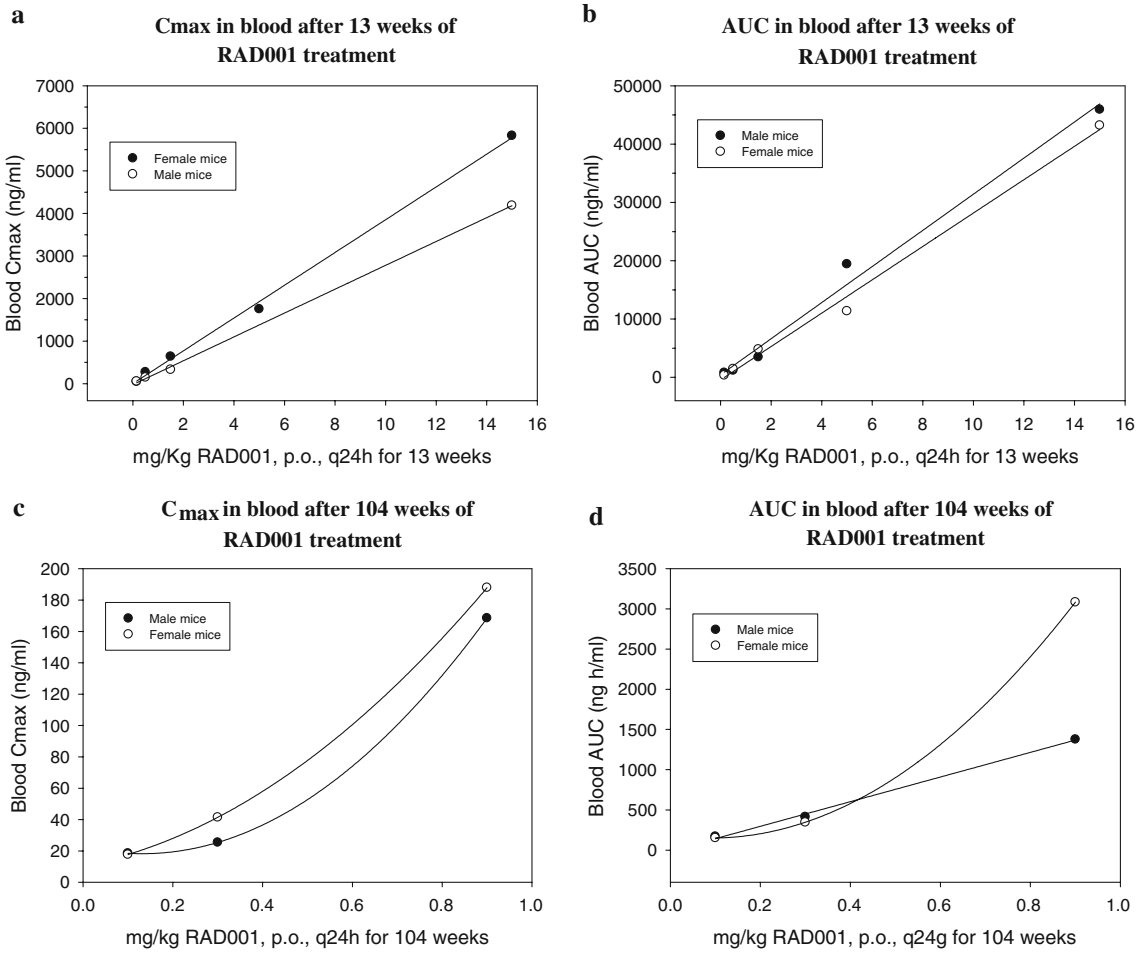

Fig. 2 PK profile of RAD001 in CD-1 mice after long-term treatment. CD-1 mice were treated with various doses of RAD001 p.o., once per day for 13 (**a**, **b**), or 104 (**c**, **d**) weeks. Two hours after the last RAD001 administration, blood samples were obtained and the concentration of RAD001 determined by HPLC–MS/MS

week regimens did not appear to predict tumor accumulation of RAD001.

RAD001 pharmacokinetics in rats

Previously, a physiologically based PK model of RAD001 in non-tumor bearing rats was derived [17], and the PK of RAD001 in tumor-bearing rats was used to develop PK–PD models aimed at designing and interpreting data from Phase I clinical trials [14, 15, 22]. In contrast to mice, rats have a lower serum protein binding (92% in rats vs. 99.9% in mice) and greater erythrocyte uptake of RAD001 (60% in rats vs. 2% in mice, see above). As discussed below, the PK of RAD001 in rats is also distinct from that occurring in mice (Table 3, Figure SM6).

Non-tumor bearing rats

RAD001 was administered once to Sprague–Dawley rats at 1.5 and 15 mg/kg, p.o., and at 1 and 10 mg/kg, i.v. Following oral administration, dose-normalized blood C_{max} values (C_{max}/D) were somewhat higher than for tumor-bearing Lewis rats (see below). Furthermore, RAD001 C_{max}/D and AUC/D values were slightly dose-under proportional by either the oral or the i.v. route. Inspection of the data also suggested $t_{1/2\ \alpha}$ of approximately 12–17 h and a $t_{1/2\beta}$ of 49–52 h (Table 3). Pairing the low-dose and high-dose AUC/D values suggested 23 and 38% oral bioavailability, respectively, of RAD001. Further calculated PK parameters based on i.v. administration included CL: 21 and 32 mL/(min kg), V_{ss}: 53 and 44 L/kg, for 1 and 10 mg/kg doses, respectively.

In Wistar rats, RAD001 levels in whole blood and various tissues were obtained 24 h after the last administration of repeated daily oral doses of 0.5 or 5 mg/kg for 14 days (Table 4, Figure SM6). K_p values were shown to be approximately dose proportional in blood, kidney, lymph nodes and lung, but an increase in tissue penetration occurred in brain, testes and skin with the higher dose of RAD001 (Table 4), similar to prior observations [17].

Table 3 Pharmacokinetic parameters of RAD001 in rats

	CA20948 pancreatic tumor xenograft-bearing Lewis rats			Non-tumor bearing Sprague–Dawley rats			
	Blood	Tumor	Heart	1.5 mg/kg, p.o.	15 mg/kg, p.o.	1 mg/kg, i.v.	10 mg/kg, i.v.
T_{max} (h)	0.5	4–8	0.5	1	2	2	2
C_{max} (ng/mL or ng/g)	212 ± 17	770 ± 17	1,755 ± 144	133 ± 3.1	189 ± 11.6	90 ± 3.8	1,347 ± 1.89
C_{max}/D	44	154	351	88.7	12.6	90.0	134.7
T_{last} (h)	72	72	72	72	72	50	50
C_{last} (ng/mL or ng/g)	3.3 ± 0.5	55 ± 7	57 ± 8	0.3 ± 0.09	2.0 ± 0.45	2.4 ± 0.13	9.4 ± 0.45
C_{min}/D	2.2	3.1	12	0.2	0.1	2.4	0.9
$t_{1/2}$ (h)	20.4	21.9	19.3	17.1 (49.7)	13.4 (59.5)	14.3 (49.2)	11.8 (54.6)
AUC (ng h/mL)	1,332	15,821	22,413	249	1,971	713	5,256
AUC/D (ng h/mL)/dose	227	3,227	4,482	166	131	713	525
$C_{max\ tissue}/C_{max\ blood}$		3.6	2.4				
AUC_{tissue}/AUC_{blood}		12.1	1.4				
Estimates using free RAD001 levels in blood							
$C_{max\ tissue}/C_{max\ blood\ (unbound)}$		338	245				
$AUC_{tissue}/AUC_{blood\ (unbound)}$		1,185	142				

Female Lewis rats bearing s.c. CA20948 pancreatic tumors of approximately 1,000 mm^3 were administered a single p.o. dose of 5 mg/kg RAD001. Whole blood and tissues were obtained at various time points following administration, and RAD001 levels determined using HPLC/MS. For p.o. administration, AUC and $t_{1/2}$ values were calculated by non-compartmental analysis of extravascular dosing (WinNonlin) using mean values. C_{max} and t_{max} were determined by inspection of the data. The data from intravenously administered RAD001 used non-compartmental modeling with vascular input. Where possible, data are expressed as mean ± SEM, $n = 4$. For Sprague–Dawley rats, the first $t_{1/2}$ represents the initial half-life during elimination phase and the number in parentheses is the terminal half-life

Table 4 RAD001 tissue levels after repeated p.o. administration to Wistar rats

Tissue	0.5 mg/kg RAD001			5 mg/kg RAD001			Fold-increase based on:		
	Tissue level (ng/mL or ng/g)	K_p (C_{tissue}/C_{blood})		Tissue level (ng/mL or ng/g)	K_p (C_{tissue}/C_{blood})		Tissue level	K_p (C_{tissue}/C_{blood})	
		Whole blood	Unbound fraction		Whole blood	Unbound fraction		Whole blood	Unbound fraction
Blood	1.1 ± 0.3			13.5 ± 1.0			12.3		
Kidney	36.3 ± 2.2	33.9	206	324.0 ± 16.2	24	159.9	8.9	1.4	1.3
Liver	27.0 ± 3.0	25.2	153	388.4 ± 34.4	28.8	191.7	14.4	0.9	0.8
Brain	4.8 ± 1.9	5.3	28	77.7 ± 5.4	19.9	38.4	16.2	0.3	0.7
Testes	5.7 ± 1.2	15	33	269.3 ± 12.5	11.2	132.9	47.2	1.3	0.2
LN	16.0 ± 1.5	61.6	91	151.4 ± 33.9	47.8	74.8	9.5	1.3	1.2
Lung	65.9 ± 3.7	0	375	645.6 ± 43.8	3.2	318.7	9.8		1.2
Skin	0.0 ± 0.0	5.3	0	43.0 ± 4.9	19.9	21.2	>43	0.3	

Wistar rats were administered RAD001 at 0.5 or 5 mg/kg, p.o., once per day for 14 days. Data represent tissue RAD001 levels 24 h after the last administration (mean ± SEM, $n = 4$). The limit of detectability was 1.0 ng/mL or 5 ng/g. The K_p values are based upon the ratio of total tissue RAD001 levels/determined RAD001 levels in blood either total or estimated unbound fraction. The unbound fractions were estimated to be 0.2 ± 0.03 at 0.5 mg/kg and 2.0 ± 0.1 at 5 mg/kg

LN lymph nodes

Metabolism in blood

In the Wistar rat, RAD001 was metabolized in whole blood, plasma and the blood cells as demonstrated by a declining ratio of RAD001 concentration/total ^3H radioactivity (Fig. 4d). After a short lag phase, RAD001 was initially metabolized in whole blood at a rate similar to that occurring in plasma, and metabolism in these compartments was much faster than the rate by isolated blood cells. Subsequently, the rate of metabolism of RAD001 in whole blood declined to become similar to the constant slower rate displayed by the blood cells. Overall, this suggests that

metabolism of RAD001 in blood is dominated by enzymes in the plasma, and partitioning of RAD001 into erythrocytes protects RAD001 from the rapid plasma metabolism.

The metabolite profiles are characterized by the presence of RAD001, and five major peaks including fatty acid conjugates, hydroxylated and hydrolytic ring lytic metabolites (data not shown, but see [31]). One day following the administration of RAD001 to rats, intact RAD001 represented the major component in blood (36–46% of the radioactivity). The major metabolite was the conjugate of RAD001 with linolic acid formed by an ester bond with the hydroxy-group of the hydroxy-ethyl side chain in position-40. Further fatty acid conjugates were esters with myristic, palmitoleic and arachidonic acid, respectively [data not shown, see 26].

Excretion in rats

Wistar rats were treated orally with [^{3}H]RAD001 (0.5 mg/kg once) and urine and feces were collected. Cumulative urine excretion accounted for 1.0 ± 0.7, 1.0 ± 0.4 and 1.0 ± 0.3% of the injected radioactivity, between 0–24, 24–48 and 48–72 h, respectively. Cumulative fecal elimination comprised 72.8 ± 7.3, 70.8 ± 7.0, and 73.8 ± 6.8%, between 0–24, 24–48 and 48–72 h, respectively. At 28 days post administration, the cumulative fecal excretion of [^{3}H]RAD001 was 90 ± 2%. At steady-state, tritiated water represented about 15% of the total radioactivity found in urine (approx. 0.1% of the dose) indicating that the position of the ^{3}H-label in RAD001 ("ring" labeled) was metabolically stable in rats (data not shown). Thus, excretion of RAD001 was almost exclusively by the fecal (bile) route.

Tumor-bearing rats

Lewis rats bearing s.c. CA20498 tumors were orally administered RAD001 (5 mg/kg once) and drug levels were determined by HPLC/MS. The compound was orally bioavailable and highly distributed to the tissues where it was detectable up to 72 h (Table 3, Figure SM6). The C_{max} (∼212 ng/mL) in blood was 0.5 h with a $t_{1/2}$ of ∼20.5 h and $AUC_{0–72h}$ of ∼1,332 ng h/mL. In heart, the C_{max} was also 1 h (∼1,755 ng/g) but was 8 h in tumor (∼717 ng/g). The $t_{1/2}$ in heart and tumor were ∼19 and ∼22 h, respectively, and the $AUC_{0–72h}$ values were ∼22,413 and ∼15,821 ng h/mL, respectively.

PK modeling in tumor-bearing rats

Through a re-iterative process, one-compartment PK models (Table SM4) were used to describe the effect of various multiple treatments on plasma and tumor PK (Figures SM8, SM9). The model predicted that 5 mg/kg RAD001, p.o. once per day, would result in blood levels after 6 days of treatment with RAD001, ∼231 ng/mL at the C_{max} and a C_{min} of 2.1 ng/mL. With this regimen, predicted tumor RAD001 levels increased such that after 6 days of treatment C_{max} and C_{min} values of ∼987 and ∼437 ng/g, were reached approximately a 1.4- and 7.9-fold increase, respectively, over the initial levels determined. Modeling of 5 or 20 mg/kg once per week predicted high C_{max} levels in plasma (∼230 and ∼917 ng/mL, respectively) and tumor (∼600 and ∼2,398 ng/mL, respectively), but very low C_{min} levels in blood and tumor (Figure SM9).

Comparison of rat and mouse tumor vascularity

The vascularity of tumors was studied non-invasively by DCE-MRI to determine plasma volume (V_p), permeability (K^{trans}) and interstitial space (V_e). The tumor burden as a percentage of body-weight was relatively small (always <2%, range 0.3–2.0), see Table 5. Two rat tumors, mammary BN472 in BN-rats and pancreatic CA20498 in Lewis rats, had significantly larger V_p (medians 4.6–4.9) than three different mouse tumors models (medians 0.6–2.0%), the exception being B16 melanoma (median 3.9%). There were less marked differences in V_e between mouse and rat tumors, but the rat tumors also had significantly greater K^{trans} compared to the three mouse tumors.

These comparisons while interesting, used different tumor types. However, when a rat pituitary GH3 cell line, was grown s.c. in both nude mice and nude rats, there were highly significant differences for all three vascular parameters with the rat tumor having >2-fold greater V_p, K^{trans} and V_e (Table 5). Taken together, the greater penetration of RAD001 in the tumors in rats maybe partially accounted for by the influence of the rat host on tumor vascularity.

Comparison of RAD001 PK in mice, rats and cancer patients

The data are summarized in Table 6. At doses considered near optimal in terms of tumor efficacy and tolerability, the C_{max} and AUC values of unbound RAD001 in humans exceeded that of tumor-bearing rats and mice. Although dose selection for cancer patients [14] was based upon modeling of the PK-PD relationship for the PD marker p70S6 kinase (S6K) in circulating blood leukocytes [9, 22], the data also suggest that based upon the preclinical efficacy models, the blood levels attained in cancer patients should be sufficient to exert an anti-tumor effect (see also Table SM5).

Table 5 Comparison of rat and mouse tumor vascularity as measured by non-invasive DCE-MRI

Host	Tumor	%TB	N	V_p (%)	K^{trans} ($s^{-1} \times 10^3$)	V_e (%)
Mouse, C57BL/6	B16/BL6	0.3 ± 0.2	31	3.8 ± 1.5 (3.9)	0.27 ± 0.24 (0.21)*#	8 ± 4 (7.0)*#
Mouse, C3H/He	RIF-1	2.0 ± 0.6	19	1.0 ± 0.4 (0.9)*#	0.12 ± 0.05 (0.12)*#	18 ± 17 (15)*
Mouse, athymic-nude	HT-29	0.4 ± 0.2	17	0.8 ± 0.7 (0.6)*#	0.36 ± 0.19 (0.29)*	15 ± 9 (16)*
Rat, Brown-Norway	BN472	0.9 ± 1.0	46	4.6 ± 1.3 (4.6)	0.62 ± 0.15 (0.63)	20 ± 4 (21)
Rat, Lewis	CA20498	0.4 ± 0.3	26	5.5 ± 2.6 (4.9)	0.43 ± 0.13 (0.41)	16 ± 16 (12)
Rat, athymic-nude	GH3	0.5 ± 0.2	8	11.2 ± 2.3 (11.6)[a]	1.04 ± 0.33 (0.96)[a]	32 ± 13 (27)[b]
Mouse, athymic-nude	GH3	1.7 ± 0.6	10	4.3 ± 2.8 (4.1)	0.38 ± 0.02 (0.35)	15 ± 7 (13)

Results show mean ± SD and in parentheses the median (two significant figures) for tumor plasma volume (V_p), permeability transfer constant (K^{trans}) and interstitial leakage space (V_e) determined by kinetic modeling of DCE-MRI data following injection of the contrast agent Vistarem (P792). Tumors were untreated and had a percentage tumor burden (%TB), i.e. tumor volume as a fraction of animal body-weight, of 0.3–2.0%. Comparisons were made using a Kruskal–Wallis one-way ANOVA on ranks with Dunn's analysis post hoc for multiple comparisons where * or # signifies significantly different ($P < 0.05$) to BN472 (*) or CA20498 (#). When the same tumor (GH3) was compared in both Harlan nude rats and Harlan nude mice, a 2-tailed t test was used ([a]$P < 0.001$; [b]$P < 0.01$)

Table 6 Comparison of some plasma (serum) PK parameters based on unbound levels of RAD001 in mice, rats and humans

Host	RAD001 dose		PK Parameter:					
			C_{max} ng/mL	C_{min} ng/mL	$AUC_{0-\infty}$	$t_{1/2}$ (h)	RBC partitioning (%)	Serum protein binding
BALB/c nude mouse	5 mg/kg, p.o.	Determined from single administration	2.5	0.1	19.0	5.4	2	99.9
	(0.125 mg per mouse)	1-compartment model, single administration	2.4	ND	20.1			
		2-compartment model, single administration	2.6	ND	21.7			
Lewis Rat	5 mg/kg, p.o.	Determined from single administration	6.8	0.1	42.6	20.4	60	92
	(1.5 mg per rat)	1-compartment model, single administration	7.8	ND	42.1			
Cancer patients[a]	5 mg	Determined after multiple administrations (steady state)	9.6	1.6	84.4	26	80	70
	10 mg		18.3	4.0	154	38		

Data for mice and rats taken from Tables 1 and 3 and in the supplementary material (Tables SM4-SM6). For mice, unbound (free) RAD001 was estimated from the measured plasma level (0.1% is unbound). For rats, unbound RAD001 was estimated from the measured blood level (60% partitioned into erythrocytes, 92% is bound)

ND not determined

[a] Human data is from O'Donell et al. [14] and the unbound serum RAD001 levels estimated as 30%

RAD001 pharmacokinetics in brain tissue of mice and rats

The blood–brain barrier restricts the entry of many anti-cancer agents and therefore limits their use against brain tumors [27, 28]. Although many factors contribute to the restricted permeability of this endothelium layer, the P-gp pump predominates and could also therefore potentially impact RAD001 efficacy since RAD001 is a P-gp substrate [16].

Non-tumor bearing athymic BALB/c mice

Orally administered RAD001 (5 mg/kg once) penetrated poorly into brain (Fig. 3), achieving a C_{max} of 69 ng/g (K_p of 44 based on C_{max}), and displaying the lowest AUC-based K_p value of 19. When based upon total RAD001 blood C_{max}, the penetration was 1.5% which was similar to the estimate based upon AUC (1.9%). However, this brain RAD001 level could be overestimated due to the blood content of the brain. The longer $t_{1/2}$ of RAD001 in brain

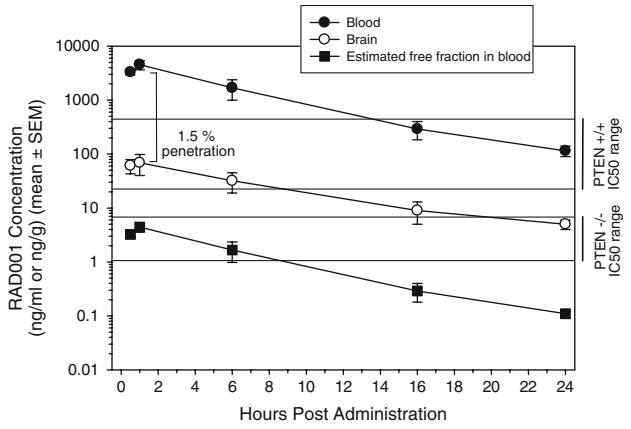

Fig. 3 RAD001 penetration into mouse brain relative to the in vitro sensitivity of glioblastoma cells. Female BALB/c athymic nude mice were administered a single p.o. administration of RAD001 AT 5 mg/kg. Plasma and brain tissue were obtained at various time points following administration, and RAD001 levels determined using HPLC/MS. Data are expressed as mean ± SEM, $n = 4$. In vitro IC_{50} data were taken from Tanaka et al. [22]. Free RAD001 levels in brain were estimated by using cellular partitioning (60% partitioning into blood) and serum protein binding coefficients (92% bound) from blood

compared to plasma, and an increased K_p based upon C_{last} determinations, suggested that RAD001 penetrated brain tissue with an intact blood–brain barrier and may accumulate upon repeated administration. Considering the free fraction of RAD001 in blood (Table 1), either the brain had an active mechanism for accumulation of RAD001 or RAD001 unbound in blood is not the only form of RAD001 that can penetrate the blood–brain barrier.

Despite the low penetration, total RAD001 levels in brain exceeded the in vitro antiproliferative IC_{50} levels for $PTEN^+$ glioblastoma cell lines for approximately 12 h post administration and for approximately 24 h for $PTEN^-$ glioblastoma cell lines (Fig. 3) [see also 22, 29].

Non-tumor bearing rats

Wistar rats received a short i.v. infusion (0.5 min) of [^{3}H]RAD001 (0.1–30 mg/kg). Brain and blood levels of total RAD001 concentration increased linearly with the dose up to 1 mg/kg and thereafter a non-linear increase was observed in both compartments (Fig. 4a). A low K_p (brain/blood concentration ratio) of 0.2–0.6 was observed within the dose range 0.1–1 mg/kg, followed by a rapid increase up to 3.1-fold at the highest dose of 30 mg/kg (Fig. 4b). The K_p values corresponding to total radioactivity concentrations differed considerably from those for total RAD001 concentration. Thus, low K_p values of roughly 0.3 obtained across the entire dose range, indicated that there was no selective uptake of the radiolabelled compound and also suggested that radioactive metabolites of RAD001 which can rapidly appear in blood do not significantly penetrate the brain. Furthermore, at this 2-h sampling time, the ratio of unchanged RAD001 to total radioactivity averaged 1.0 within the whole dose range, indicating that drug taken up by the brain is not subject to rapid metabolism (data not shown).

The time dependency (0–168 h) of RAD001 levels in brain and whole blood levels of RAD001 and radioactivity observed after an i.v. bolus of 1 mg/kg are displayed in Fig. 4c. The time profile of brain concentrations of RAD001 indicated rapid uptake followed by a slow efflux. At 168 h post-dose, significant brain levels of 6 ng/g were still observed whereas no significant blood levels were detected. The concentration profile of RAD001 in brain compared with that of radioactivity suggests that once bound in the brain the parent drug is less subject to metabolism. In the time period 0.08–24 h, the ratio of unchanged RAD001 to total radioactivity in brain averaged 1.0, thus demonstrating the absence of metabolites in the brain during the first 24 h post RAD001 administration. This is in dramatic contrast to the blood, where rapid metabolism of RAD001 occurs, largely within the plasma compartment (Fig. 4d). However, at 168 h post administration, metabolites of [^{3}H]RAD001 represented 60% of brain radioactivity. Given the slow reduction in ^{3}H radioactivity in the brain over time, this suggests efflux of the metabolites (and RAD001) is slow (data not shown).

Discussion

Rats, and in particular mice, have been extensively used to profile RAD001. Previous published data [e.g. 9–11] (and the present study) indicate that RAD001 is orally active in mice, and the present study showed an approximately 12% oral bioavailability. A recently published pharmacokinetic study using Swiss mice [30] showed that RAD001 dosed at 0.25 mg/kg had a plasma $t_{1/2}$ of 4 h, a C_{max}/dose 80 ng/ml and an AUC/dose of 512 ng h/mL/dose, decidedly lower than those described here, with a T_{max} of 3 h; a slower absorption that determined here. Chu et al. [30] used a commercially available tablet formulation of RAD001 (Certican®) which was ground and dispersed in water at a final concentration of 10 mg/ml. In contrast, our study used a microemulsion formulation which apparently facilitated greater gastrointestinal absorption. This emphasizes the dramatic effect that formulation can have on rodent pharmacokinetics.

The present study also documents high tissue penetration (despite high binding to plasma proteins of 99.9%) and slow elimination of RAD001 from the tissues (notably tumor) in mice. This profile is distinct from that of rats which have a higher bioavailability (23–38%), higher

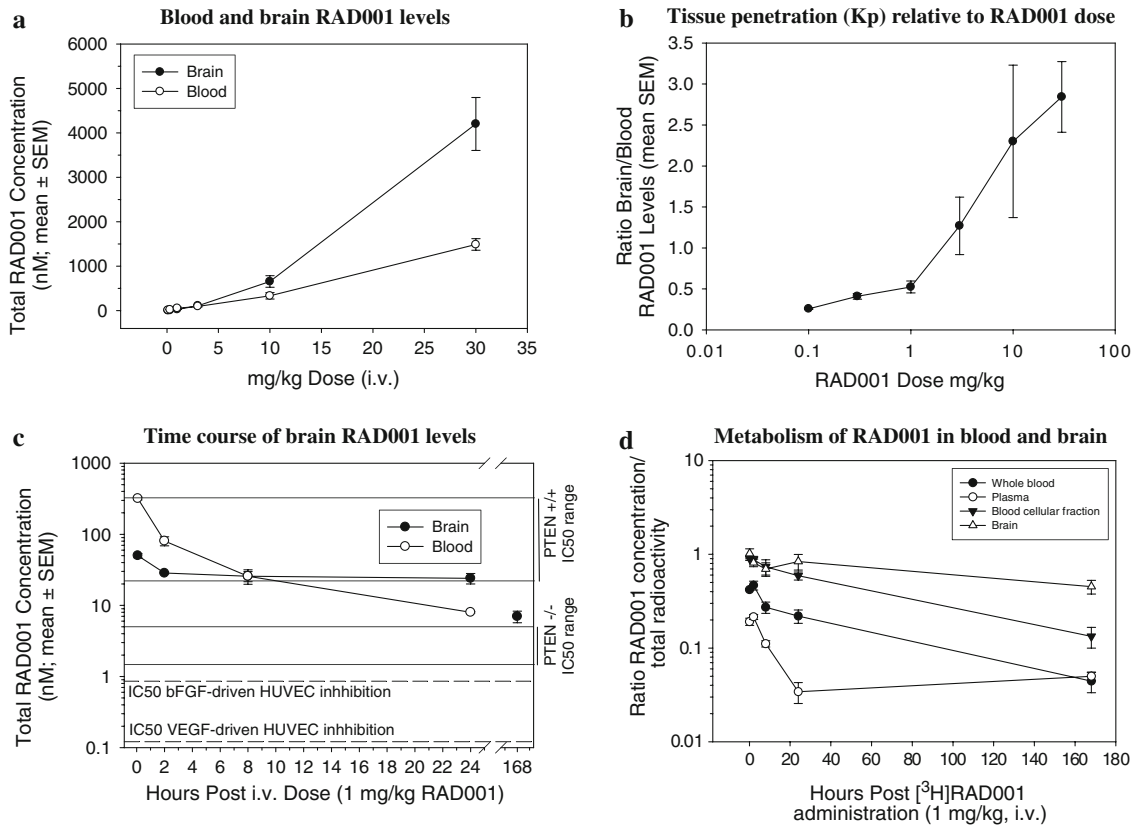

Fig. 4 Dose-dependent uptake and metabolism of RAD001 in rat brain. Male Wistar rats were administered RAD001 p.o., once at the doses indicated and the blood and brain RAD001 levels determined for samples obtained 2 h post administration (**a**), and tissue penetration (K_p) as a function of RAD001 dose calculated (**b**). In **c**, RAD001 blood and brain tissue levels were determined at various times following a single 1 mg/kg i.v. administration. In **d**, the ratio of RAD001 and total ^{3}H radioactivity were determined at various times following a single 1 mg/kg i.v. administration of [^{3}H]RAD001

partitioning into erythrocytes (60%) and significantly lower binding to plasma proteins (92%). Excretion is similar in both species, with the fecal route being dominant. It has been reported that first-pass metabolism of RAD001 involves both the intestine and liver [31], and suggests that liver impairment, which is common during cancer, will affect RAD001 pharmacokinetics. Despite mice having a larger blood AUC/mg/kg dose (nude mouse = 3,883 and Lewis rat = 227 ng h/(mL mg kg) dose), rats have a greater volume of distribution (V_{ss} 44–53 L/kg compared with 0.42 L/kg for mice) for RAD001, and consequently there was an overall greater tissue penetration of RAD001 in rats than mice. Owing to the dramatic differences in RAD001 protein binding between these species, there were many tissues with similar extents of tissue penetration when based upon unbound (free) fraction in blood. Both species demonstrated increased K_p values over time indicating greater retention of RAD001 in tissues over that in blood. As it is the unbound drug that likely will act on solid tumors, such differences in protein binding and tissue penetration will influence anti-tumor effect. Furthermore, mice and rats differed dramatically with respect to tumor uptake of RAD001 (non-compartmental, AUC_{0-72h}/dose in mouse = 516 and rat = 3,227 ng h/kg/dose). This may be partially explained by the two to three-fold greater plasma volume (V_p) and permeability of rat tumors compared to mouse tumors. The V_p values in rats (2–11%) were similar to those measured in the gliomas of 18 patients also using the DCE-MRI method where a median of 4% was recorded [32]. This data again highlights greater similarity between humans and rats and suggests that the higher vascularity of rat tumors may facilitate greater RAD001 uptake by the tumors; an effect that may occur with other compounds as well.

RAD001 is apparently retained and/or accumulated in tumor tissue and this may contribute to the observed efficacy of once daily administration, despite the relatively low blood/plasma levels at the end of a single treatment. Given that RAD001 is present in tumor tissue at 24 h post administration, this would suggest that once daily dosing would result in accumulation of RAD001 in tumor (and other) tissues, that may then exceed the IC_{50} of tumor cells within a few days. PK modeling suggested that tumor accumulation of RAD001 would occur upon multiple

administration, resulting in about two-fold higher level in mice and about 7.9-fold in rats than that following a single administration. However, modeling less frequent (once per week) administration of higher doses (5 or 20 mg/kg RAD001) indicated little or no accumulation in tumor and plasma.

At efficacious doses, RAD001 presents a characteristic PK profile in experimental animals. If this can be attained in humans, there can be some degree of confidence that the therapy will also possess some degree of antitumor effect in cancer patients. Our data suggest this was the case, since at the efficacious dose of 5 mg/kg, p.o., the C_{max} and AUC of unbound RAD001 in plasma attained by mice are considerably lower than that of humans receiving daily doses of 5 or 10 mg [14], whereas in rats, these parameters are closer to those attained in cancer patients. The human RAD001 PK profile produces unbound drug levels that exceed those predicted to be attained by a ED50 doses of RAD001 for antitumor activity in mice and rats, it is likely that these RAD001 doses used in humans will exert an antitumor effect; an hypothesis supported, for example, by tumor responses recorded in metastatic renal cell carcinoma [13].

Due to their sensitivity to RAD001 [1, 9, 22], gliomas may be a good target tumor for RAD001 treatment. In both mice and rats, RAD001 penetrated poorly brain tissue with an intact blood–brain barrier. However, once in the brain, RAD001 had a long $t_{1/2}$ and, at least in rats, was slowly metabolized. Since RAD001 remains in the brain until the time of the next administration, it could be that the compound accumulates there, although this may depend on the dose since low-dose RAD001 (0.9 mg/kg, p.o., daily) did not result in accumulation upon repeated administration. Indeed, uptake of RAD001 into the brain was highly dose-dependent, with an inflexion point occurring between 1 and 10 mg/kg. The increase in K_p values observed at higher doses is consistent with the hypothesis of a saturation of an efflux pump present in the brain capillary endothelial cells. Despite low brain penetration, daily administration of RAD001 led to levels in the brain, which exceeded the in vitro antiproliferative, IC_{50} levels of glioblastoma cell lines for up to 24 h. Consequently, in patients, accumulation of RAD001 in brain (and other) tissues may exceed antiproliferative concentrations within a few days. Furthermore, the antiangiogenic action of RAD001 [6] would also contribute to its activity in the brain, since gliomas for example are highly vascularised and respond well to antiangiogenic agents [33, 34]. Thus, although daily administration has been adopted as the preferred regimen for RAD001 in the clinic [14, 15], high-dose, once-weekly RAD001 or a hybrid weekly/daily administration regimen should be considered for clinical testing against tumors in the brain given that this regimen may increase brain penetration.

In conclusion, the PK of RAD001 differed markedly between mice and rats, with rats having a PK profile closer to that of humans. RAD001 can penetrate the brain in both animal models but high intermittent doses may be more appropriate for the treatment of experimental brain tumors and this principle may also extend to the clinic.

Acknowledgments M. Lemaire, J. Figueiredo, G. Kraus and H. Kaufmann are thanked for their input in obtaining part of the data. Melanie Muller, Marc Hattenberger, Julianne Vaxelaire, and Stephane Ferretti provided excellent technical assistance.

References

1. Boulay A, Lane HA (2007) The mammalian target of rapamycin kinase and tumor growth inhibition. Recent Results Cancer Res 172:99–124
2. Albanell J, Dalmases A, Rovira A, Rojo F (2007) mTOR signalling in human cancer. Clin Transl Oncol 9:484–493
3. Guertin DA, Sabatini DM (2007) Defining the role of mTOR in cancer. Cancer Cell 12:9–22
4. Abraham RT, Eng CH (2008) Mammalian target of rapamycin as a therapeutic target in oncology. Expert Opin Ther Targets 12:209–222
5. Jiang BH, Lui LZ (2008) Role of mTOR in anticancer drug resistance: perspectives for improved drug treatment. Drug Resist Updat 11:63–76
6. Lane HA, Wood JM, McSheehy PM, Allegrini PR, Boulay A, Brueggen J, Littlewood-Evans A, Maira SM, Martiny-Baron G, Schnell CR, Sini P, O'Reilly T (2009) Evaluation in vitro and in vivo of the anti-angiogenic/anti-vascular properties of the mTOR inhibitor RAD001 (everolimus) has antiangiogenic/vascular properties distinct from a VEGFR tyrosine kinase inhibitor. Clin Cancer Res 15:1612–1622
7. Shinohara ET, Cao C, Niermann K, Mu Y, Zeng F, Hallahan DE, Lu B (2005) Enhanced radiation damage of tumor vasculature by mTOR inhibitors. Oncogene 24:5414–5422
8. Beuvink I, Boulay A, Fumagalli S, Zilbermann F, Ruetz S, O'Reilly T, Natt F, Hall J, Lane HA, Thomas G (2005) The mTOR inhibitor RAD001 sensitizes tumor cells to DNA-damaged induced apoptosis through inhibition of p21 translation. Cell 120:747–5938
9. Boulay A, Zumstein-Mecker S, Stephan C, Stephan C, Beuvink I, Zilbermann F, Haller R, Tobler S, Heusser C, O'Reilly T, Stolz B, Marti A, Thomas G, Lane HA (2004) Antitumor efficacy of intermittent treatment schedules with the rapamycin derivative RAD001 correlates with prolonged inactivation of ribosomal protein S6 kinase 1 in peripheral blood mononuclear cells. Cancer Res 64:252–261
10. Mabuchi S, Altomare DA, Cheung M, Zhang L, Poulikakos PI, Hensley HH, Schilder RJ, Ozols RF (2007) Testa JR (2007) RAD001 inhibits human ovarian cancer cell proliferation, enhances cisplatin-induced apoptosis, and prolongs survival in an ovarian cancer model. Clin Cancer Res 13:4261–4270
11. Mabuchi S, Altomare DA, Connolly DC, Klein-Szanto A, Litwin S, Hoelzle MK, Hensley HH, Hamilton TC, Testa JR (2007) RAD001 (Everolimus) delays tumor onset and progression in a transgenic mouse model of ovarian cancer. Cancer Res 67:2408–2413
12. Awada A, Cardoso F, Fontaine C et al (2008) The oral mTOR inhibitor RAD001 (everolimus) in combination with letrozole in

patients with advanced breast cancer: results of a phase I study with pharmacokinetics. Eur J Cancer 44:84–91
13. Motzer RJ, Escudier B, Oudard S, Hutson TE, Porta C, Bracarda S, Grünwald V, Thompson JA, Figlin RA, Hollaender N, Urbanowitz G, Berg WJ, Kay A, Lebwohl D, Ravaud A; RECORD-1 Study Group (2008) Efficacy of everolimus in advanced renal cell carcinoma: a double-blind, randomised, placebo-controlled phase III trial. Lancet 372(9637):449–456
14. O'Donnell A, Faivre S, Burris HA, Rea D, Papadimitrakopoulou V, Shand N, Lane HA, Hazell K, Zoellner U, Kovarik JM, Brock C, Jones S, Raymond E, Judson I (2008) I.Phase I pharmacokinetic and pharmacodynamic study of the oral mammalian target of rapamycin inhibitor everolimus in patients with advanced solid tumors. J Clin Oncol 26:1588–1595
15. Tabernero J, Rojo F, Calvo E, Burris H, Judson I, Hazell K, Martinelli E, Ramon y Cajal S, Jones S, Vidal L, Shand N, Macarulla T, Ramos FJ, Dimitrijevic S, Zoellner U, Tang P, Stumm M, Lane HA, Lebwohl D, Baselga J (2008) Dose- and schedule-dependent inhibition of the mammalian target of rapamycin pathway with everolimus: a phase I tumor pharmacodynamic study in patients with advanced solid tumors. J Clin Oncol 26:1603–1610
16. Crowe A, Bruelisauer A, Duerr L, Guntz P, Lemaire M (1999) Absorption and intestinal metabolism of SDZ-RAD and rapamycin in rats. Drug Metab Dispos 27:627–632
17. Laplanche R, Meno-Tetang GML, Kawai R (2007) Physiologically based pharmacokinetic (PBPK) modeling of everolimus (RAD001) in rats involving non-linear tissue uptake. J Pharmacokinet Pharmacodynam 34:373–400
18. Kirchner GI, Meier-Wiedenbach I, Manns MP (2004) Clinical pharmacokinetics of everolimus. Pharmacokinet 43:83–95
19. Kovarik JM, Beyer D, Bizot MN, Jiang Q, Allison MJ, Schmouder RL (2005) Pharmacokinetic interaction between verapamil and everolimus in healthy subjects. Br J Clin Pharmacol 60:434–437
20. Kovarik JM, Kaplan B, Tedesco Silva H, Kahan BD, Dantal J, Vitko S, Boger R, Rordorf C (2002) Exposure-response relationships for everolimus in de novo kidney transplantation: defining a therapeutic range. Transplantation 73:920–925
21. Fouladi M, Laningham F, Wu J, O'Shaughnessy MA, Molina K, Broniscer A, Spunt SL, Luckett I, Stewart CF, Houghton PJ, Gilbertson RJ, Furman WL (2007) Phase I study of everolimus in pediatric patients with refractory solid tumors. J Clin Oncol 25:4806–4812
22. Tanaka C, O'Reilly T, Kovarik JM, Shand N, Hazell K, Judson I, Raymond E, Zumstein-Mecker S, Stephan C, Boulay A, Hattenberger M, Thomas G, Lane HA (2008) Identifying optimal biologic doses of everolimus (RAD001) in patients with cancer based on the modeling of preclinical and clinical pharmacokinetic and pharmacodynamic data. J Clin Oncol 26:1596–1602
23. Weidensteiner C, Rausch M, McSheehy PM, Allegrini PR (2006) Quantitative dynamic contrast-enhanced MRI in tumor-bearing rats and mice with inversion recovery TrueFISP and two contrast agents at 4.7 T. J Magn Reson Imaging 24:646–656
24. Ebenhan T, Honer M, Amethamey S, Schubiger P, Becquet M, Ferretti S, Cannet C, Rausch M, McSheehy P (2009) Comparison of [18F]-tracers in various experimental tumour models by PET imaging and identification of an early response biomarker for the novel microtubule stabiliser patupilone. Mol Imaging Biol (published on-line, May 2009)
25. Ludden TM, Beal SL, Sheiner LB (1994) Comparison of the Akaike Information Criterion, the Schwarz Criterion and the F-test as guides to model selection. J Pharmacokinet Biopharm 22:431–445
26. Boernsen KO, Egge-Jacobsen W, Inverardi B, Strom T, Streit F, Schiebel HM, Benet LZ, Christians U (2007) Assessment and validation of the MS/MS fragmentation patterns of the macrolide immunosuppressant everolimus. J Mass Spectrom 42:793–802
27. Blakeley J (2008) Drug delivery to brain tumors. Curr Neurol Neurosci Rep 8:235–241
28. de Vries NA, Beijnen JH, Boogerd W, van Tellingen O (2006) Blood-brain barrier and chemotherapeutic treatment of brain tumors. Expert Rev Neurother 6:1199–1209
29. Yang L, Clarke MJ, Carlson BL, Mladek AC, Schroeder MA, Decker P, Wu W, Kitange GJ, Grogan PT, Goble JM, Uhm J, Galanis E, Giannini C, Lane HA, James CD, Sarkaria JN (2008) PTEN loss does not predict for response to RAD001 (Everolimus) in a glioblastoma orthotopic xenograft test panel. Clin Cancer Res 14:3993–4001
30. Chu C, Abbara C, Noël-Hudson MS, Thomas-Bourgneuf L, Gonin P, Farinotti R, Bonhomme-Faivre L- (2009) Disposition of everolimua in mdr1a-/mdr1b mice and after a pre-treatment of lapatinib in Swiss mice. Biochem Pharmacol 77:1629–1634
31. Yokomasu A, Yano I, Sato E, Masuda S, Katsura T, Inui K (2008) Effect of intestinal and hepatic first-pass extraction on the pharmacokinetics of everolimus in rats. Drug Metab Pharmacokinet 22:469–475
32. Harrer JU, Parker GJ, Haroon HA, Buckley DL, Embelton K, Roberts C, Balériaux D, Jackson A (2004) Comparative study of methods for determining vascular permeability and blood volume in human gliomas. J Magn Reson Imaging 20:748–757
33. Fisher MJ, Adamson PC (2002) Anti-angiogenic agents for the treatment of brain tumors. Neuroimaging Clin N Am 12:477–499
34. Folkerth RD (2000) Descriptive analysis and quantification of angiogenesis in human brain tumors. J Neurooncol 50:165–172